Theoretical Chemistry Accounts (2018) 137:174
https://doi.org/10.1007/s00214-018-2376-z

REGULAR ARTICLE

Modeling induction phenomena in amino acid cation–π interactions

Chetan Raj Rupakheti[1] · Benoît Roux[1,2] · François Dehez[3] · Chris Chipot[3,4,5]

Received: 29 June 2018 / Accepted: 25 September 2018 / Published online: 15 November 2018

Abstract
Cation–π interactions are widely recognized as an important class of interactions, notably in biology and supramolecular chemistry, participating in molecular recognition and association phenomena. Numerical simulations relying on additive force fields perform usually poorly in modeling precisely these interactions. It is now well established that accurate reproduction of the interaction energy of a positively charged group bound to the π-electron cloud of an aromatic ring requires an explicit treatment of induction effects by means of polarizable potentials. In this contribution, we compare critically the ability of the CHARMM Drude polarizable force field to describe a series of prototypical cation–π interactions observed in proteins with that of the pairwise additive CHARMM36 force field. Toward this end, potentials of mean force characterizing the binding of amino acid side-chain models, namely ammonium and guanidinium cations, on the one hand, and toluene, para-cresol and 3-methylindole, on the other hand, have been determined within the extended adaptive biasing force framework.

Keywords Recognition and association · Polarization · Free energy · Molecular simulations

1 Introduction

Over thirty years ago, cation–π interactions were recognized as a fourth actor in molecular recognition and association phenomena, in addition to the three other common non-covalent interactions, namely hydrogen bonds, salt bridges and hydrophobic effect [1]. Owing to their short-range nature, it is tempting to regard them as unconventional hydrogen bonds [2], considering that the latter usually form between a donor and a π-electron density, which, in the absence of lone pairs, acts as an acceptor [3]. The seminal work of Kebarle and coworkers brought to light the duality of electrostatic and polarization contributions as the driving force for the binding of a potassium ion to a benzene ring. From a phenomenological standpoint, cation–π interactions arise from the superimposition of two effects of a different nature. The electric field generated by the cation polarizes the π-electron

Published as part of the special collection of articles In Memoriam of János Ángyán.

Electronic supplementary material The online version of this article (https://doi.org/10.1007/s00214-018-2376-z) contains supplementary material, which is available to authorized users.

✉ François Dehez
francois.dehez@univ-lorraine.fr

✉ Chris Chipot
chipot@ks.uiuc.edu

Chetan Raj Rupakheti
rupakhetic@uchicago.edu

Benoît Roux
chipot@ks.uiuc.edu

[1] Department of Biochemistry and Molecular Biology, Gordon Center for Integrative Science, University of Chicago, Chicago, Illinois 60637–1454, United States

[2] Leadership Computing Facility, Argonne National Laboratory, 9700 Cass Avenue, Building 240, Argonne, Illinois 60439–8643, United States

[3] Laboratoire International Associé Centre National de la Recherche Scientifique et University of Illinois at Urbana-Champaign, Unité Mixte de Recherche no 7019, Université de Lorraine, B.P. 70239, 54506 Vandœuvre-lès-Nancy cedex, France

[4] Theoretical and Computational Biophysics Group, Beckman Institute for Advanced Science and Technology, University of Illinois at Urbana-Champaign, 405 North Mathews Avenue, Urbana, Illinois 61801, United States

[5] Department of Physics, University of Illinois at Urbana-Champaign, 1110 West Green Street, Urbana, Illinois 61801, United States

cloud of the aromatic compound, which corresponds to an r^{-2} interaction. In turn, the induced dipole moment of the ring interacts with the polarizing charge through its electrostatic potential, which also corresponds to an r^{-2} interaction. Identification of new non-covalent interactions in simple cation–π complexes was rapidly followed by a host of investigations in biological objects, wherein unusual hydrogen bonds formed between amino and aromatic moieties had long been observed [4–6]. Cation–π interactions have proven strong enough to compete with the hydration of charged, titratable species and promote binding in the hydrophobic pocket of a protein lined with aromatic residues [7–9]. Ubiquitous to a host of components of the cell machinery, they have been proposed to be responsible for the binding of acetylcholine, one of the most extensively studied neurotransmitters, to acetylcholinesterase [10, 11]. Extensive analyses of the protein data bank, or PDB [12], have highlighted a preference for tryptophan to be engaged in an interaction with a cationic amino acid, among which arginine dominates over both lysine and the protonated form of histidine [8]. These analyses have also revealed a pronounced anisotropy of the non-covalent interaction formed by aromatic and cationic side chains, whereby the latter approaches the π-electron cloud in the direction normal to it [13]. In stark contrast to salt bridges, the strength of which is modulated by the dielectric permittivity of the environment, cation–π interactions can sustain exposure to the aqueous surroundings and are, therefore, commonly observed at the surface of proteins [14]. Though cation–π interactions appear to not be pivotal for the stability of proteins [15, 16], they could, nevertheless, participate in their folding [7]. In fact, proximity of a basic, titratable side chain from an aromatic one induces a bias in the local geometry toward the formation of a non-covalent interaction [8].

At the conceptual level, cation–π interactions result from the attraction of a polarizing, positively charged moiety toward the quadrupole engendered by the π-electron cloud of a noteworthily polarizable aromatic ring [7, 9, 17, 18]. Owing to the large polarizability of aromatic species and the strong polarization exerted by the cation, faithful depiction of cation–π interactions falls out of the scope of rudimentary, pairwise additive potential energy functions, which only account for induction phenomena in an average sense [19–21]. The attractive part of the short-range potential describing induction effects, which formally ought to be represented analytically by means of an r^{-4} term [13, 22], is clearly absent from minimalist force fields devoid of an explicit treatment of polarization. Pioneering molecular mechanics-based calculations on prototypical cation–π complexes have emphasized the necessity to incorporate induction phenomena to recover the expected attractive feature of the intermolecular potential, in particular in aqueous environments [23, 24]. One possible route to handle polarization explicitly in numerical simulations, notably in molecular dynamics (MD) simulations, consists in introducing Drude oscillators, formed by auxiliary particles carrying a partial charge and tethered to real atoms by means of a harmonic spring [25, 26]. In response to the local electric field felt by the polarizable sites of the molecule, these auxiliary particles move relative to the real atoms as their respective charge varies, resulting in an overall self-consistent reorganization of the charge distribution induced by the chemical environment. The main advantage of this approach lies in its conceptual simplicity, compared to more sophisticated representations of the induction energy by means of a multipole expansion [27], allowing MD simulations to remain in the framework of a point-charge model, thus limiting the computational overhead incurred in the explicit treatment of polarization [28].

In the present contribution, we probe the ability of two academic force fields to describe the cation–π interaction formed in an aqueous environment between model basic and aromatic amino acid side chains, using high-performance geometric free energy calculations [29]. Specifically, the reversible association of guanidinium and ammonium, on the one hand, with toluene, para-cresol and 3-methylindole, on the other hand, is examined through potential of mean force (PMF) calculations with a potential energy function resting on a two-body additive approximation, and another one accounting for non-additive induction effects by means of classical Drude oscillators [26].

2 Methods

Computational assays In this study, toluene, para-cresol and 3-methylindole serve as proxies for the side chain of phenylalanine, tyrosine and tryptophan, whereas guanidinium and ammonium represent the cationic moiety of arginine and lysine, respectively. Each molecular assembly consisted of an aromatic compound and a cation solvated in a thermalized bath of 1958 water molecules, corresponding to six independent computational assays of dimensions approximately equal to $38 \times 38 \times 38$ Å^3. For the MD simulations performed with a non-additive force field, the ancillary virtual particles and lone pairs of electronegative elements [30] were added to the computational assays using the CharmmGUI server [31].

Molecular dynamics simulations All MD simulations presented herein were carried out with the parallel, scalable program NAMD 2.12 [32]. For the simulations wherein induction phenomena were neglected, the TIP3P model [33] and the CHARMM general force field [34] (CGenFF) were used to describe water and the amino acid side-chain models, respectively. Conversely, for the simulations accounting for mutual polarization, the SWM4-NDP model [35] and the

CHARMM Drude force field [36, 37] were employed for water molecules and the side-chain proxies, respectively. It ought to be mentioned here that the parameters of the non-additive CHARMM potential energy function were taken "out of the box," without any changes. Further refinement could be introduced through the introduction of additional terms or NBFIX corrections [38]. The r–RESPA multiple time-step algorithm [39] was employed to integrate the equations of motion with a time step of 2 and 4 fs for short- and long-range interactions, respectively, in all simulations using a two-body additive force field, and with a time step of 0.5 fs in all simulations involving Drude particles. The SETTLE algorithm was used to constrain the covalent bonds of water molecules to their equilibrium length [40]. Covalent bonds of the side-chain models involving hydrogen atoms were constrained to their equilibrium length by means of the RATTLE algorithm [41]. The temperature and the pressure were maintained at 298 K and 1 atm, respectively, using Langevin dynamics and the Langevin piston method [42]. Long-range electrostatic forces were taken into account by means of the particle mesh Ewald algorithm [43]. A cutoff of 12 Å was utilized to truncate van der Waals and short-range Coulombic interactions. Periodic boundary conditions (PBCs) were applied in the three directions of Cartesian space. Visualization and analyses of all MD trajectories were performed with the VMD program [44].

Free energy calculations The extended adaptive biasing force algorithm [45–47] was employed to determine the PMFs, $w(r)$, that underlie cation–π reversible association, through integration of the average force exerted along the transition coordinate, r. Under these premises, a biasing force is estimated such that, once applied onto the relevant atoms, it yields a Hamiltonian bereft of an average force acting along the transition coordinate, defined here as the Euclidian distance, r, separating the center of mass of the cation, i.e., the nitrogen atom of ammonium, or the carbon atom of guanidinium, from the centroid of the π-electron cloud. The reaction pathway spanning 13 Å, i.e., $2 \leq r \leq 15$ Å, was not stratified into non-overlapping windows and was discretized in bins 0.1 Å wide, wherein samples of the local force acting along r were accumulated. Analyses of the PDB have revealed a marked preference of the cation to approach the aromatic ring in the direction normal to its plane [13, 24]. For this reason, the PMFs were determined enforcing a series of geometric restraints with harmonic potentials centered at $\theta = 90°$ (see Fig. 1). In this event, the cation is able to rotate unhindered about the axis perpendicular to the π–electron cloud. In particular, ammonium can adopt freely a mono-, bi- or tridentate orientation, whereas, for guanidinium, two $-NH_2$ groups approach the aromatic ring. Determination of each PMF required 100 ns of sampling, representing an aggregate time of 600 ns for the present computational investigation.

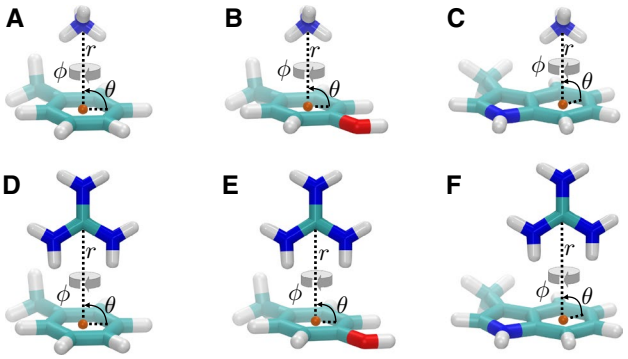

Fig. 1 Reversible association of amino acid side-chain models: ammonium:toluene (**a**), ammonium:para-cresol (**b**), ammonium:3-methylindole (**c**), guanidinium:toluene (**d**), guanidinium:para-cresol (**e**) and guanidinium:3-methylindole (**f**). r denotes the transition coordinate defined as the Euclidian distance between the center of mass of the cation, i.e., the nitrogen atom of ammonium, or the carbon atom of guanidinium, and the centroid of the π–electron cloud. Geometric restraints are enforced on angle θ to ensure perpendicular approach of the cation toward the aromatic ring. The cation can, however, rotate freely about angle ϕ

3 Results

To achieve a fair comparison of the additive CHARMM36 and the non-additive CHARMM Drude force fields, it should be stressed that the latter employed in this study consists of the original version developed by Roux and coworkers for modeling amino acids in the condensed phase [36, 37] and, thus, has not been specifically refined against cation–π reference complexes. Lamoureux and coworkers derived a series of ad hoc Lennard-Jones parameters to model more accurately cation–π interactions in the framework of the Drude force field [37, 48, 49]. Their strategy relies on the addition of an extra Lennard-Jones site located at the centroid of the six-membered ring.

The PMFs evaluated for both the additive CHARMM36 and the non-additive CHARMM Drude force fields are reported in Fig. 2. In all cases, two free energy minima can be observed, namely a contact minimum, where the cation interacts directly with the aromatic moiety, and a solvent-separated minimum, in which the cation–π interaction is mediated by a water molecule. It has been shown previously that occurrence of the second minimum is linked to the restriction of the binding process along the C_6 symmetry axis of the aromatic ring [24]. When cation binding is averaged over all possible orientations, the solvent-separated minimum usually vanishes [24, 49]. Depending on the cation and the π–electron cloud, the first minimum lies between 2.8 and 4 Å, whereas the second minimum emerges between 5.6 and 6.9 Å. For some complexes, explicit inclusion of polarization affects the position of the minima, an observation in line with the findings of Khan et al. [50].

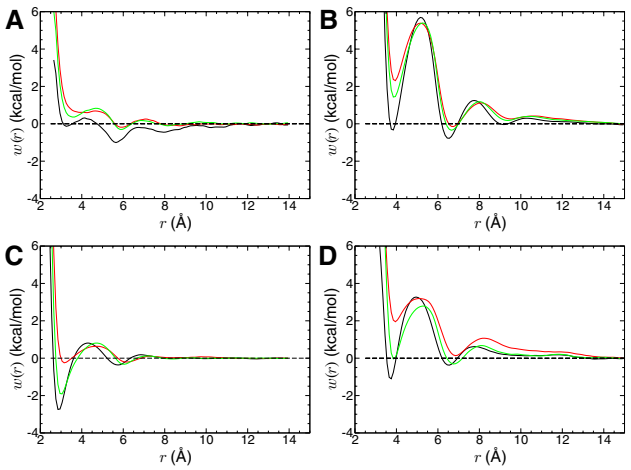

Fig. 2 Potentials of mean force characterizing the reversible association of amino acid side-chain models. Ammonium–π PMFs determined with a two-body pairwise (**a**) and non-additive (**c**) force field. Guanidinium–π PMFs determined with a two-body pairwise (**b**) and non-additive (**d**) force field. Color coding for the aromatic compounds: 3-methylindole (black line), para-cresol (red line) and toluene (green line). The transition coordinate, r, is defined in Fig. 1. All the PMFs obey the classical definition [51], whereby $\lim_{r\to\infty} w(r) := 0$, and thus include the Jacobian term $2r/\beta$ in the gradient of the free energy

Additive CHARMM36 force field For toluene and para-cresol interacting with ammonium and guanidinium, the PMFs obtained with the standard CHARMM36 force field (Fig. 2a, 2b) reveal that, compared to the dissociated state, the contact minimum is predicted to be less stable by 0.3 to 0.6 kcal/mol and 1.4 to 2.3 kcal/mol, for ammonium and guanidinium, respectively. Concerning the solvent-separated minimum, the free energy difference with the dissociated complex is nearly zero. At slight variance with toluene and para-cresol, 3-methylindole described by the pairwise additive force field has a contact minimum corresponding to the same free energy as the dissociated complex, and a solvent-separated minimum favored by 0.8 to 1.0 kcal/mol for both cations. The main difference between the profiles obtained with ammonium or guanidinium is rooted in the free energy barrier separating the two minima, ranging from 0 to 0.5 kcal/mol for the former cation and from 3 to 6 kcal/mol for the latter. Interestingly enough, a similar trend was observed over twenty years ago for ammonium axially constrained along the C_6 symmetry axis of the toluene aromatic ring, using a different academic pairwise additive force field [24].

Non-additive CHARMM Drude force field Resorting to the CHARMM Drude polarizable force field essentially results in lowering the free energy of the contact minima for all complexes, compared to the pairwise additive description, while leaving the depth of the solvent-separated minima globally unchanged (see Fig. 2c, d). As the cation, either ammonium or guanidinium, approaches the π–electron cloud of the aromatic compound, the auxiliary Drude particles attached to the latter move with respect to the real atoms, resulting in an induced dipole ranging at the contact minimum between 0.2 and 0.4 D for toluene and para-cresol, respectively. For para-cresol, explicit description of polarization shifted down the contact minima by 1.0 to 1.5 kcal/mol, compared with the CHARMM36 pairwise additive force field, corresponding to the same free energy as the solvent-separated minima and the dissociated state for ammonium, albeit leaving the situation qualitatively unchanged for guanidinium—i.e., contact > solvent-separated ≈ dissociated state. At variance with the pairwise additive description, the intimate pair formed by toluene and ammonium is predicted by the Drude force field to be more stable than its dissociated state with a free energy difference of 1.9 kcal/mol. For the guanidinium:toluene complex, the contact and the solvent-separated binding motifs are as probable as the dissociated state. The main quantitative and qualitative difference between the additive and the non-additive description is observed for cation:3-methylindole complexes. The use of Drude particles predicts the contact complexes to be the most stable conformation with a free energy of 2.8 and 1.9 kcal/mol for the ammonium and the guanidinium cations, respectively.

When compared to quantum chemical calculations in the gas phase, standard pairwise additive force fields are prone to underestimate grossly the gas-phase interaction energies of cation–π complexes [13, 19, 24, 50]. It should be emphasized here that empirical force fields are tailored to describe the condensed phase and, thus, confronting their relative ability to predict gas-phase quantities, compared to ab initio calculations, is somewhat unfair. One possible way to recover the correct gas-phase cation–π interaction energy in vacuum consists in fine-tuning the Lennard-Jones contribution to the additive force fields either through reparametrization [50], or by introducing an ad hoc function, for instance, by means of a 10–12 or a 4–12 potential [13, 24]. Another strategy toward the accurate description of cation–π systems consists in introducing an explicit polarization term in the potential energy function by means of Drude particles [37, 49, 52], or more elaborate polarizable models relying, for example, on charge flow and dipole polarizabilities [19, 20, 53, 54].

Experiments carried out in an aqueous medium usually predict binding affinities for cation–π complexes much lower than those computed in the gas phase. This apparent discrepancy is now well understood, and the effect of the solvent on the strength of cation–π complexes has been quantified by theoretical calculations [55]. In light of drug-binding experiments, it was shown that cation–π interactions enhance the free energy of association by nearly 3 kcal/mol [9, 56]. CHARMM36 pairwise additive force field is clearly not able to account for such a stabilization free energy. It chiefly

predicts a dissociation for the various cation–π complexes examined here, or slightly favors the solvent-separated minimum by less than 1 kcal/mol for 3-methylindole complexes. Resorting to the CHARMM Drude force field improves the description for 3-methylindole and toluene interacting with ammonium and guanidinium, but leaves the situation essentially unchanged for those complexes involving para-cresol. The effect of explicit polarization further depends on the nature of the cation. When ammonium is the polarizing cation, wherein the charge is rather well localized, the Drude model predicts a binding affinity of 1.9 and 2.8 kcal/mol for toluene and 3-methylindole, respectively. In sharp contrast, for guanidinium, the CHARMM Drude force field leads to a binding affinity of 1.1 kcal/mol for 3-methylindole, but fails to describe for toluene a contact minimum more stable than the dissociated state.

Evidence of cation–π interaction in an aqueous environment is documented in the literature. Lamoureux et al. report a free energy minimum of about −3.5 kcal/mol, inferred from their PMF for the ammonium:toluene complex, using optimized CHARMM Lennard-Jones parameters [49]. Similarly, Chipot et al. report a free energy minimum of −5.5 kcal/mol for the same complex, employing an ad hoc corrective potential in the AMBER force field [24]. Experimental estimates of the association constant for a related cation–π complex have also been reported by Schneider et al. [57], ranging between 2.7 and 3.3 M^{-1}. In stark contrast to the above PMF calculations, wherein the approach of the cation toward the π–electron cloud is geometrically restrained along the normal to the latter, experimental measurements of the binding affinity reflect an orientationally averaged cation–π association. In addition, Dougherty et al. have estimated the interaction energy of methyl ammonium and benzene in water to be on the order of −5.5 kcal/mol, and from their survey of PDB complexes, they have observed that energetically favorable cation–π interactions are rarely completely buried within proteins, but prefer instead to be solvent-exposed [8, 14].

To check whether the interaction with the solvent is the source of the discrepant PMFs for toluene and para-cresol, we computed the corresponding free energy profiles in vacuum. The minimum for para-cresol is about −17.5 kcal/mol, and that for toluene is about −21 kcal/mol. Both minima are found around 2.9 Å in vacuum. It should be noted that the presence of the solvent clearly reduces the cation–π binding by nearly 17 kcal/mol for para-cresol and 19 kcal/mol for toluene. However, we observed a similar trend for the two PMFs (in water and in vacuum), hence suggesting that the discrepant results are rooted primarily in the intermolecular forces in the cation–π complexes.

To identify the differences in the free energy profiles, we also performed an interaction energy calculation in vacuum for the ammonium:para-cresol and ammonium:toluene pairs at their equilibrium distance determined from the PMFs. A 1-ns trajectory formed of 2000 snapshots was generated for each cation–π pair. The average interaction energy was -29.1 ± 1.6 and -34.8 ± 1.6 kcal/mol for the ammonium:para-cresol and ammonium:toluene complex, respectively. The interaction energy follows a similar trend, compared to the free energy, suggesting that the origin of the discrepant results stems from the electrostatic term of the potential energy function.

The partial-charge distribution of toluene and para-cresol atoms reinforces this observation. The partial charge on the carbon atom connected to the hydroxyl group is + 0.297 e.c.u. (electron charge unit) in para-cresol, whereas the same carbon atom in the toluene ring has a partial charge of −0.133 e.c.u. The presence of a positive charge in the para-cresol ring, thus, weakens the molecular quadrupole of the latter, and leads to a reduced interaction with ammonium.

4 Conclusion

From the results of the present contribution, it is clear that introducing explicit polarization by means of a set of Drude particles globally enhances the description of cation–π complexes, compared to a pairwise additive force field. Yet, describing the subtle balance within the intermolecular forces responsible for the recognition and association of cations to aromatic compounds by means of cost-effective polarizable models still remains a daunting challenge. Orabi and Lamoureux were able to recover systematically consistent binding affinities for various cation–π pairs, using an optimized version of the CHARMM Drude force field [49]. Toward this end, they corrected the original polarizable potential energy function, following a strategy akin to that employed for additive force fields [13, 24, 50], namely through fine-tuning of the Lennard-Jones interaction potential by means of ad hoc functionals or parameters handled using the NBFIX facility of the CHARMM36 force field. This strategy has, however, limitations of its own. First, the parametrization strongly depends on the level of theory of the quantum mechanical calculations and on the basis set employed to compute the reference quantities. Orabi and Lamoureux resorted to the standard 6–311++G(*d*,*p*) basis set, which has proven suboptimal in quantifying electric properties, compared to specialized basis sets, e.g., Sadlej, ELP [58, 59]. Moreover, such a reparametrization approach lacks generality, as it requires the optimization of specific pairs of Lennard-Jones parameters for every cation–π complexes, while introducing an additional interaction site at the center of the aromatic ring. This scheme may not be easily extended to anion–π complexes, wherein large penetration and exchange induction effects have proven difficult to capture [20]. Last, cation–π pairing represents one possible

association mode in proteins, but more sophisticated binding motifs, such as cation–π–cation trimers, are also frequently observed. The parameters calibrated for dimers may not necessarily transfer in a straightforward fashion to a trimeric organization. Put together, our data suggest that, while explicit inclusion of induction phenomena definitely improves the description of cation–π interactions, even when in the absence of an ad hoc reparametrization, there is still room for improvement toward reproducing systematically the subtle balance of the intermolecular forces at play.

Acknowledgements The authors gratefully acknowledge fruitful exchanges with Javier Luque (Universidad de Barcelona, Spain) over the years. This work was supported by the National Institutes of Health (through Grant No. NIGMS-2R01 GM-072558) and by the Prof@Lorraine initiative of the University of Lorraine.

References

1. Sunner J, Nishizawa K, Kebarle P (1981) J Phys Chem 85:1814
2. Deakyne CA, Meot-Ner M (Mautner) (1985) J Am Chem Soc 107:474
3. Legon AC, Millen DJ (1987) Acc Chem Res 20:39
4. Perutz MF, Fermi G, Abraham DJ, Poyart C, Bursaux E (1986) J Am Chem Soc 108:1064
5. Burley SK, Petsko GA (1986) FEBS Lett 203:139
6. Levitt M, Perutz MF (1988) J Mol Biol 201:751
7. Dougherty DA (1996) Science 271:163
8. Gallivan JP, Dougherty DA (1999) Proc Natl Acad Sci USA 96:9459
9. Dougherty DA (2013) Acc Chem Res 46:885
10. Dougherty DA, Stauffer DA (1990) Science 250:1558
11. Sussman JL, Harel M, Frolow F, Oefner C, Goldman A, Toker L, Silman I (1991) Science 253:872
12. Berman HM, Westbrook J, Feng Z, Gilliland G, Bhat TN, Weissig H, Shindyalov IN, Bourne PE (2000) Nucleic Acids Res 28:235
13. Minoux H, Chipot C (1999) J Am Chem Soc 121:10366
14. Gallivan JP, Dougherty DA (2000) J Am Chem Soc 122:870
15. Flocco MM, Mowbray SL (1994) J Mol Biol 235:709
16. Mitchell JBO, Nandi CL, McDonald IK, Thornton JM, Price SL (1994) J Mol Biol 239:315
17. Kumpf RA, Dougherty DA (1993) Science 261:1708
18. Mecozzi S, West AP Jr, Dougherty DA (1996) Proc Natl Acad Sci USA 93:10566
19. Dehez F, Soteras I, Luque FJ, Ángyán J, Schulten K, Chipot C (2007) J Chem Theory Comput 3:1914
20. Archambault F, Chipot C, Gutiérrez IS, Luque FJ, Schulten K, Dehez F (2009) J Chem Theor Comput 5:3022
21. Luque FJ, Dehez F, Chipot C, Orozco M (2011) Wires Comput Mol Sci 1:844
22. Stone AJ (1996) The theory of intermolecular forces. Clarendon Press, Oxford
23. Caldwell JW, Kollman PA (1995) J Am Chem Soc 117:4177
24. Chipot C, Maigret B, Pearlman DA, Kollman PA (1996) J Am Chem Soc 118:2998
25. Lamoureux G, Roux B (2003) J Chem Phys 119:3025
26. Lemkul JA, Huang J, Roux B, MacKerell AD (2016) Chem Rev 116:4983
27. Stone AJ (1985) Mol Phys 56:1065
28. Jiang W, Hardy DJ, Phillips JC, Mackerell AD Jr, Schulten K, Roux B (2011) J Phys Chem Lett 2(2):87
29. Chipot C (2014) Wiley Interdiscip Rev Comput Mol Sci 4:71
30. Huang J, Lopes PEM, Roux B, MacKerell AD Jr (2014) J Phys Chem Lett 5:3144
31. Jo S, Kim T, Iyer VG, Im W (2008) J Comput Chem 29:1859
32. Phillips JC, Braun R, Wang W, Gumbart J, Tajkhorshid E, Villa E, Chipot C, Skeel L, Kalé RD, Schulten K (2005) J Comput Chem 26:1781
33. Jorgensen WL, Chandrasekhar J, Madura JD, Impey RW, Klein ML (1983) J Chem Phys 79:926
34. Vanommeslaeghe K, Hatcher E, Acharya C, Kundu S, Zhong S, Shim J, Darian E, Guvench O, Lopes P, Vorobyov I, Mackerell AD Jr (2010) J Comput Chem 31:671
35. Lamoureux G, MacKerell AD Jr, Roux B (2003) J Chem Phys 119:5185
36. Lopes PEM, Lamoureux G, Roux B, Mackerell AD (2007) J Phys Chem B 111:2873
37. Orabi EA, Lamoureux G (2012) J Chem Theory Comput 8:182
38. MacKerell AD Jr, Bashford D, Bellott M, Dunbrack RL Jr, Evanseck JD, Field MJ, Fischer S, Gao J, Guo H, Ha S, Joseph-McCarthy D, Kuchnir L, Kuczera K, Lau FTK, Mattos C, Michnick S, Ngo T, Nguyen DT, Prodhom B, Reiher WE III, Roux B, Schlenkrich M, Smith JC, Stote R, Straub J, Watanabe M, Wiórkiewicz-Kuczera J, Yin D, Karplus M (1998) J Phys Chem B 102:3586
39. Tuckerman ME, Berne BJ, Martyna GJ (1992) J Phys Chem B 97:1990
40. Miyamoto S, Kollman PA (1992) J Comput Chem 13:952
41. Andersen HC (1983) J Comput Phys 52:24
42. Feller SE, Zhang YH, Pastor RW, Brooks BR (1995) J Chem Phys 103:4613
43. Darden TA, York DM, Pedersen LG (1993) J Chem Phys 98:10089
44. Humphrey W, Dalke A, Schulten K, Molec J (1996) Graphics 14:33
45. Comer J, Gumbart JC, Hénin J, Lelièvre T, Pohorille A, Chipot C (2015) J Phys Chem B 119:1129
46. Fu H, Shao X, Chipot C, Cai W (2016) J Chem Theory Comput 12:3506
47. Lesage A, Lelièvre T, Stoltz G, Hénin J (2017) J Phys Chem B 121:3676
48. Wang L (2012) Annu Rev Biochem 81:615
49. Orabi EA, Lamoureux G (2018) J Phys Chem B 122:2251
50. Khan HM, Grauffel C, Broer R, MacKerell AD, Havenith RWA, Reuter N (2016) J Chem Theory Comput 12:5585
51. Chandler D (1987) Introduction to modern statistical mechanics. Oxford University Press, Oxford
52. Lamoureux G, Orabi EA (2012) Mol Sim 38:704
53. Soteras I, Curutchet C, Bidon-Chanal A, Dehez F, Ángyán J, Orozco M, Chipot C, Luque FJ (2007) J Chem Theory Comput 3:1901
54. Ansorg K, Tafipolsky M, Engels B (2013) J Phys Chem B 117:10093
55. Xu J, Voth GA (2005) Proc Natl Acad Sci U S A 102(19):6795
56. Anderson MA, Ogbay B, Arimoto R, Sha W, Kisselev OG, Cistola DP, Marshall GR (2006) J Am Chem Soc 128:7531
57. Schneider HJ, Schiestel T, Zimmermann P (1992) J Am Chem Soc 114:7698
58. Celebi N, Ángyán JG, Dehez F, Millot C, Chipot C (2000) J Chem Phys 112:2709
59. Chipot C, Dehez F, Ángyán JG, Millot C, Orozco M, Luque FJ (2001) J Phys Chem A 105:11505